Preclinical evaluation of ^{213}Bi-labeled plasminogen activator inhibitor type 2 in an orthotopic murine xenogenic model of human breast carcinoma

Tamantha K. Stutchbury,[1] Fares Al-ejeh,[1] Gillian E. Stillfried,[1] David R. Croucher,[1] John Andrews,[2] David Irving,[3] Matthew Links,[4] and Marie Ranson[1]

[1]School of Biological Sciences, University of Wollongong, Wollongong, New South Wales, Australia; [2]JLA Bioprocess Consulting, Berowra, New South Wales, Australia; [3]Diabetes Vaccine Development Centre, c/- School of Population Health, University of Melbourne, Melbourne, Victoria, Australia; and [4]Cancer Care Centre and University of New South Wales Clinical School, St. George Hospital, Sydney, New South Wales, Australia

Abstract

Tumor-associated urokinase plasminogen activator (uPA) is a critical marker of invasion and metastasis, has strong prognostic relevance, and is thus a potential therapeutic target. Experimental data published to date has established the proof-of-principle of uPA targeting by ^{213}Bi-labeled plasminogen activator inhibitor type 2 (α-PAI-2) in multiple carcinoma models. Here, we present preclinical toxicologic and efficacy assessment of α-PAI-2 in mice, using both single and multiple-dose schedules, administered by an i.p. route. We also present novel data showing that human PAI-2 inhibited murine uPA and was specifically endocytosed by murine fibroblast cells. This diminishes potential problems associated with species specificity of the targeting reagent in toxicologic assessments as human α-PAI-2 should interact with any uPA-expressing host cells. In this model, single bolus doses up to 36 mCi/kg α-PAI-2 did not reach the maximum tolerated dose (MTD). The MTD for a multiple fractionated (once daily for 5 days) administration schedule was determined to lie between 4.8 and 6.0 mCi/kg/d $\times$ 5. Comparison of the tumor growth rates and survival using sub-MTD single and multiple-dose schedules in an orthotopic human breast carcinoma xenograft murine model indicated that 4.8 mCi/kg/d $\times$ 5 was the most efficacious schedule. In conclusion, we have determined a safe dose and schedule of α-PAI-2 administration in mice, thus confirming that it is an efficacious therapeutic modality against tumor growth. This will allow detailed safety evaluation in a second species and for the initiation of human studies. [Mol Cancer Ther 2007;6(1):203–12]

Introduction

The inappropriate expression and activation of the urokinase plasminogen activator (uPA) system is strongly associated with tumor invasion and metastasis and has a major effect on clinical outcomes (1–6). In this system, uPA binds to its specific receptor (uPAR) and efficiently converts plasminogen into the broad-spectrum protease plasmin, which promotes cell invasion and metastasis by directly and indirectly degrading extracellular matrix (1, 2). The proteolytic activity and turnover of uPA is regulated by plasminogen activator inhibitor types 1 and 2 (PAI-1 and PAI-2; SerpinE1, SerpinB2, respectively; refs. 7–9). PAI-1 and uPA, via uPAR, can also alter cellular adhesion and migration properties through mechanisms independent of proteolysis (10).

Clinically, uPA/PAI-1 is the only biomarker that has level one evidence as a prognostic marker in early breast cancer and for predicting resistance to hormone therapy in advanced breast cancer (3, 11). These data are strongest for breast cancer but there is good evidence for prognostic significance in multiple tumor types (3). Furthermore, localization studies indicate that quiescent, normal, or benign tissues do not express significant levels of uPA/uPAR or PAI-1 compared with invasive carcinoma and metastases (2). Depending on the carcinoma type, components of the uPA system are often expressed by tumor stromal cells (4) that may be highly supportive of the tumor (12, 13).

The uPA system thus represents an accessible target for therapeutic intervention. Not surprisingly, there has been a concomitant rapid expansion in the number of studies using novel uPA-targeted therapeutic strategies (14), the majority of which are based on small-molecule uPA inhibitors and uPAR-binding antagonists (3, 4). To be clinically useful, these compounds not only have to be specific but also have to be highly stable *in vivo* as they need to elicit a continuous inhibitory effect. To this end, protein-based cytotoxin targeting strategies are attractive because their larger size enables improved pharmacokinetic properties, while specifically delivering toxic payloads to targeted cells (15). We have used a novel approach to target metastatic tumor cells based on the nontoxic, specific

Received 5/9/06; revised 10/11/06; accepted 11/16/06.

Grant support: National Health and Medical Research Council Development grant 213119 and an Australian Postgraduate Award (F. Al-ejeh, G.E. Stillfried, and D.R. Croucher).

The costs of publication of this article were defrayed in part by the payment of page charges. This article must therefore be hereby marked *advertisement* in accordance with 18 U.S.C. Section 1734 solely to indicate this fact.

Note: Current address for F. Al-ejeh: Experimental Therapeutics Laboratory, Hanson Institute, Frome Road, Adelaide, SA 5000, Australia.

Requests for reprints: Marie Ranson, School of Biological Sciences, University of Wollongong, Wollongong, NSW 2522, Australia. Phone: 61-2-42213291; Fax: 61-2-42214135. E-mail: mranson@uow.edu.au

doi:10.1158/1535-7163.MCT-06-0264

uPA-inhibitory properties of recombinant human PAI-2, which can be labeled with the cytotoxin ^{213}Bi, an α-emitting radioisotope (α-PAI-2; ref. 16). α-PAI-2 was shown to specifically kill uPA-expressing tumor cells *in vitro* in a dose-dependent manner (16, 17) and to be efficacious in preliminary studies using mouse models of human tumors (17, 18). Radio-iodinated PAI-2 has also been shown to localize in human colorectal uPA-expressing tumor xenografts in nude mouse models (19), thus providing proof-of-principle data for the uPA-targeting capability of PAI-2. Given that the efficient and rapid inhibition of carcinoma cell surface uPAR bound uPA by PAI-2 results in specific receptor-mediated endocytosis of the uPAR/uPA/PAI-2 complex (8, 20), PAI-2 is thus efficiently and specifically able to deliver and concentrate attached cytotoxins within targeted cells. As α-emitting radionuclides emit particles with a very high linear energy transfer (~100 keV/μm) but short path length of 1 to 2 cell diameters (21), only the targeted cell and possibly its immediate neighboring cells would be killed.

We have previously undertaken detailed pharmacokinetic and biodistribution analyses of PAI-2 in mice with and without tumors (19). The focus of this study was to determine a safe and efficacious dose schedule of α-PAI-2 against orthotopic human breast carcinoma xenograft growth in mice. We also present data to show that the xenogenic murine model is useful for the preclinical analysis of human α-PAI-2 because PAI-2 has the potential to interact with both host uPA-expressing and human tumor cells. This minimizes issues associated with species specificity during the toxicologic assessment of α-PAI-2. These data support the initiation of a detailed safety evaluation in a second species and future human studies.

Materials and Methods

Cell Lines and Animals

MDA-MB-231 human breast carcinoma and L929 mouse fibroblast cell lines were cultured in RPMI 1640 supplemented with 5% heat-inactivated FCS at 37°C with a 5% CO_2/95% atmosphere (22). Expression of cell surface uPAR and uPA was verified by indirect immunofluorescence using dual-color flow cytometry as described (23). Female Arc(s)nu/nu mice, ages 4 to 5 weeks, were purchased from the Animal Resources Centre (Canning Vale, WA, Australia) and were housed in a ventilated storage cabinet under positive pressure in autoclaved filter-top cages. The University of Wollongong Animal Ethics Committee approved all animal experimentation.

Orthotopic Breast Carcinoma Xenograft Model

To establish orthotopic breast carcinoma xenografts, single cell suspensions of subconfluent cultures of MDA-MB-231, prepared at a concentration of 1×10^6 cells/100 μL in PBS, were injected into each of the mammary fat pads of the first pair of nipples of mice. Cell preparations with >90% viability resulted in an 85% likelihood of each animal developing tumors (data not shown). For ''early'' tumor xenograft models, the tumor cells were allowed to grow for 1 week after cell implantation before further treatments. At this stage, tumors were not visible or palpable. ''Established'' tumor xenograft models were obtained by allowing 3 weeks for the implanted tumor cells to grow before further treatments. By this time, most tumors were small but palpable (mean ± SE tumor volume, 26 ± 7 mm^3).

Kinetic Analysis of PAI-2 Inhibition of Soluble uPA from Various Species

Association rate constants for the inhibition of human, mouse, and rabbit uPA with human recombinant 47 kDa PAI-2 (PAI-2 Pty Ltd., Australia) were determined by kinetic and fluorimetric assays, using the substrate ZGGRAMC (Sigma-Aldrich Chemical Co., St. Louis, MO) at 0.4 mmol/L in 20 mmol/L Tris, 150 mmol/L NaCl (pH 7.4) with 0.1% gelatin, using a BioTek FL500 plate reader with excitation at 360 nm and emission at 460 nm. Data were analyzed for equation fit using KaleldaGraph (Abelbeck Software, Reading, PA). Inhibition kinetics used the integrated form of the association rate equation (24) with the assumption of complete inhibition at steady-state conditions. To ensure pseudo–first-order kinetics, the enzyme concentrations, determined by active-site titration with the irreversible inhibitor Glu-Gly-Arg-chloromethyl ketone (Calbiochem, Germany), were used at <1 nmol/L.

PAI-2/uPAR Pull-Down and PAI-2 Internalization Assays

The interaction of human recombinant PAI-2 with receptor-bound murine uPA on mouse L929 fibroblast cells was verified using a biotinylated PAI-2 pull-down assay. Briefly, L929 and MCF-7 (human breast carcinoma positive control) cell monolayers were preincubated for 15 min in the absence or presence of receptor-associated protein (RAP; 200 nmol/L). RAP is a specific ligand of low-density lipoprotein receptor family members and is used to block other potentially interacting ligands with low-density lipoprotein receptors (20). After washing, the cells were incubated in the absence (negative control) or presence of 10 nmol/L biotinylated PAI-2 in ice-cold binding buffer for 1 h. Following this, the cells were washed twice, lysed by incubation for 20 min on ice with lysis buffer (150 mmol/L NaCl, 50 mmol/L Tris-HCl, 1% Triton-X100, 1% sodium deoxycholate, and 1 mmol/L $CaCl_2$), and centrifuged at 10,000 × *g* for 5 min at 4°C. After a preclearing step using agarose beads, the resulting cleared lysate supernatant was incubated with 50 μL streptavidin-agarose beads for 1 h on ice with shaking. Following this, the beads were extensively washed and bound proteins were eluted by boiling in nonreducing sample buffer and then analyzed by 12% SDS-PAGE and subsequent Western blotting using anti-uPAR rabbit polyclonal antibody (which recognizes both human and mouse uPAR; American Diagnostica, Inc., Stamford, CT). To confirm human PAI-2 endocytosis by L929 cells, we used PAI-2 labeled with $Alexa_{488}$ fluorochrome and a polyclonal antibody to quench $Alexa_{488}$ fluorescence as previously described (20). This assay is based on the protection of internalized PAI-2/$Alexa_{488}$ fluorescence from quenching by the intact membrane of viable cells.

Radiolabeling of PAI-2-Diethylenetriaminetriacetic Acid with ^{213}Bi

Recombinant human PAI-2 was conjugated with cyclic diethylenetriaminepentaacetic acid [PAI-2-diethylenetriaminetriacetic acid conjugate (PAI-2-DTTA); ref. 16]. Actinium-225 generators (U.S. Department of Energy) were prepared and washed as previously described (16), and ^{213}Bi was eluted into 0.2 mol/L citrate buffer (pH 5.5) containing 1× PBS. PAI-2-DTTA was then added at a ratio of 1 μg protein to 3 μCi (111 kBq) ^{213}Bi (unless specified otherwise) and reacted at room temperature for 5 min, forming PAI-2-DTTA-^{213}Bi (referred to as α-PAI-2). The percentage of incorporation of ^{213}Bi was determined as described by Ranson et al. (16) and was routinely obtained at >90% incorporation. In some experiments, the specific activity of α-PAI-2 was varied and the effect on protein structural integrity and ability to form SDS-stable complexes with uPA as well as cell cytotoxicity *in vitro* were assessed as previously described (16).

α-PAI-2 Administration

All α-PAI-2 and control preparations were adjusted to a final volume of 200 μL using the buffer control [0.06 mol/L HI, 0.2 mol/L citrate buffer (pH 5.5), and 1× PBS] and administered to mice by an i.p. route. Similar patterns of [^{125}I]PAI-2 biodistribution in nude mice were observed by i.p., i.v., or s.c. administration (19), indicating that the former is a suitable surrogate route for systemic administration of α-PAI-2 in these small animal models. The radioactivity of each injection preparation was measured using an Atomlab 100 Dose Calibrator (Protronic Technologies, Victoria, Melbourne, Australia) immediately before and following i.p. administration. Radioactivity remaining in syringes after administration was negligible, confirming that >95% of radioactivity was successfully administered. The actual dose of α-activity each animal received in mCi/kg (equivalent to 37 MBq/kg) was calculated based on the total dose administered (corrected for the ^{213}Bi/^{198}Au calibration factor as previously described in ref. 25) and the mouse weight.

Toxicity Studies for Determination of Maximum Tolerated Dose in Mice

The dose-tolerance relationship was examined in nude mice for a single bolus or multiple fractionated (once daily for 5 consecutive days) administration schedule of α-PAI-2 compared with control treatments. This was done using a dose-escalation protocol noting the onset of dose-limiting toxicity defined as end points of either 15% loss of body weight or distressed behavior (i.e., loss of appetite and activity, hunched posture). Animal weights were compared with day 0 (first day of treatment administration) to determine percentage weight change. Mice were sacrificed at either 20% weight loss from day 0 or at the end of the observation period, whichever arose first. The maximum tolerated dose (MTD) was defined as the highest dose at which one third of the cohort reached dose-limiting toxicity end points (26).

After administration of α-PAI-2 or control treatments, mice were closely monitored and weighed daily for 7 days, then on days 10 and 14, and twice weekly until end points were reached or until the end of the observation period, which did not exceed 90 days. At this stage, the animals were euthanized (overdose of inhaled CO_2) and the internal organs were macroscopically examined for signs of toxicity. Because previous studies found no toxicity associated with the targeting agent PAI-2 (7, 17, 18) and biodistribution of the radiolabeled compound to major organs was limited to the kidneys and liver (19), histologic assessments were restricted to these organs and one lymphoid organ, the spleen. Blood smears were taken and blood was also collected into K3 EDTA and Z serum gel minicollect tubes (Greiner Bio-one) for hematology and serum blood biochemistry to complete the toxicologic assessment. Blood biochemistry, hematology, and histopathology of animal organs and professional analyses were undertaken by an accredited animal pathology laboratory (ICP Firefly Pty Ltd., Sydney, Australia or IDEXX Laboratories, Sydney, Australia).

Efficacy Studies Using Early and Established Human Breast Carcinoma Xenograft Models

Nude mice bearing early or established breast carcinoma xenografts (see above) underwent i.p. administration of α-PAI-2 or various control treatments using either the single-dose or multiple-fractionated-dose administration schedules as described in the toxicity studies. Animals were also monitored and weighed as described in the toxicity studies. Once a tumor was visible (~5 mm at the longest diameter), it was measured twice weekly using calipers along the x and y plane of the tumor. Tumor volume was determined using the formula volume = $a \times (b^2)/2$, where a is the largest diameter and b is the smallest diameter. Tumor volume in both mammary fat pads was calculated and the values were combined to give a combined tumor volume for each animal. Antitumor assessment of treatments was determined by reduction in tumor growth rate compared with controls as determined by tumor volume and effect on overall survival.

In addition to the experimental end points outlined above, the efficacy experiment end points were defined as a tumor size of 15 × 15 mm along the longest axes or that impeded animal movement, and/or end of observation period (up to 90 days). At this stage, animals were euthanized and dissected, and major organs were removed, weighed, and examined as described above. Tumors were excised, washed, weighed, and fixed for 24 h in 10% neutral-buffered formalin. After embedding in paraffin, the tissues were sectioned and stained for uPA antigen or with H&E and examined macroscopically by a pathologist.

Statistical Analyses

All graphs were created using GraphPad Prism (version 4). Combined tumor volumes and weight changes were compared using a Student's t test (JMP version 5.1). Survival curves were analyzed by the Kaplan-Meier log-rank test (GraphPad Prism version 4). Animals that reached the end of the observation period without reaching survival end points were censored in statistical analysis of survival. $P < 0.05$ was considered statistically significant.

Results

Validation of the Xenogenic Cancer Mouse Model for Preclinical Analysis

Tumors xenografted into the mammary fat pads of mice using human MDA-MB-231 express human uPA and uPAR (4, 27). As previously shown (28), we found heterogeneous human uPA immunoreactivity in sections of the tumor xenografts and the overall degree of staining varied between individual tumors (Fig. 1A). Host stromal cells within the xenografts also stained positive for mouse uPA (Fig. 1B). Given the presence of stromal cell uPA/uPAR within the tumor xenografts, and that various murine tissues may also express uPA/uPAR (4, 29), we examined the relative species specificity of human recombinant PAI-2 to better appraise α-PAI-2–mediated toxicity and efficacy using murine xenograft models. As previously shown (7), human PAI-2 is a highly efficient and fast inhibitor of soluble human uPA (second-order rate constant of $3.6 \pm 0.5 \times 10^6$ L mol^{-1}s^{-1}). Interestingly, human PAI-2 inhibited rabbit and murine uPA with second-order association rate constants of $2.4 \pm 0.1 \times 10^6$ and $5.1 \pm 1.1 \times 10^4$ L mol^{-1}s^{-1}, respectively. Although, human PAI-2 was a comparatively less efficient inhibitor of murine uPA, this reaction rate is still considered fast and, not surprisingly, human uPA was able to form SDS-stable complexes with mouse uPA (data not shown). In addition, using uPA/uPAR–expressing murine fibroblast L929 cells as a model host fibroblast stromal cell, human PAI-2 was endocytosed in a RAP-sensitive manner by these cells (Fig. 1C). The ability of human PAI-2 to interact with uPA/uPAR on the L929 cells and human carcinoma cells, previously shown to internalize PAI-2 in a RAP- and uPA/uPAR–dependent manner (8, 20), was confirmed using a pull-down assay (Fig. 1C, *inset*).

Effect of α-PAI-2–Specific Activity

Using the citrate buffer system, PAI-2-DTTA can be reproducibly labeled with ^{213}Bi at a ratio of 0.3 to 30 μCi/μg with >90% incorporation within 5-min incubation at room temperature (data not shown). Furthermore, incorporated ^{213}Bi was strongly chelated because a maximum of 15% of

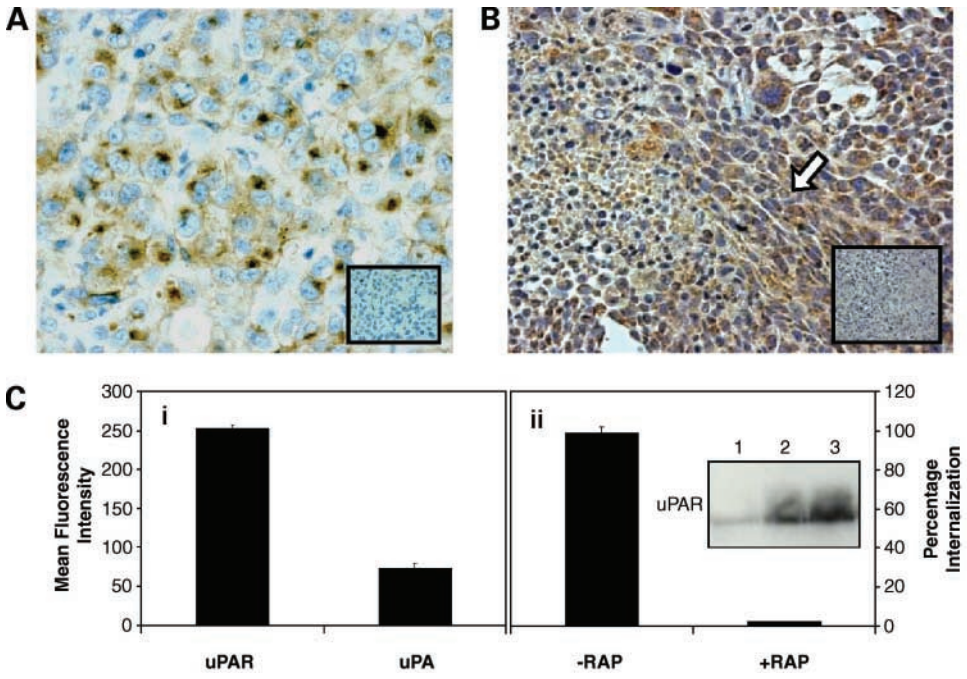

Figure 1. **A** and **B,** heterogenous expression of uPA in human MDA-MB-231 breast carcinoma xenografts excised from nude mice. Four-micrometer paraffin sections of human breast carcinoma xenografts were subjected to heat-induced antigen retrieval under high pH conditions and blocked with 10% normal horse serum. Sections were incubated with (**A**) 7.5 μg/mL mouse anti-human uPA monoclonal antibody (American Diagnostica), (**B**) 10 μg/mL rabbit anti-mouse uPA polyclonal antibody (Molecular Innovations, Inc., Southfield, MI; recognizes both human and murine uPA), or mouse/rabbit IgG isotype control (*inset*), washed and incubated with appropriate biotinylated secondary antibodies. ABC reagent and 3,3′-diaminobenzidine substrate were used to detect the antigens as per manufacturer's instructions (Vector Laboratories, Burlingame, CA). Tissue sections were counterstained with Mayer's hematoxylin. Both tumor and stromal cells display positive staining for uPA (*brown*). *Arrow,* tumor cells surrounded by stromal cells. **C,** human PAI-2 is endocytosed by murine fibroblasts. **i,** cell surface expression of uPA and uPAR by mouse L929 fibroblasts was verified by dual-color flow cytometry using anti-uPA and anti-uPAR polyclonal antibodies. *Columns,* mean ($n = 3$); *bars,* SE. **ii,** human PAI-2 is endocytosed by L929 cells in a specific manner as determined by the fluorescence quenching internalization assay. Attached L929 cells were preincubated for 15 min in the absence (−*RAP*) or presence (+*RAP*) of RAP before incubation with PAI-2/Alexa488. Following this, the cell monolayers were washed, detached, and resuspended in ice-cold binding buffer in the presence of anti-Alexa 488 polyclonal antibody and analyzed by flow cytometry. Percentage internalization was determined by dividing the fluorescence due to internalized PAI-2 in the presence of RAP by the total amount of internalized PAI-2 in the absence of RAP. *Columns,* mean ($n = 3$); *bars,* SE. *Inset,* biotinylated human PAI-2 bound to the cell surface pulled down murine uPAR from L929 cells (*lane 2*) and human uPAR from MCF-7 cells (*lane 3*), compared with a lysate only (no PAI-2) control (*lane 1*).

^{213}Bi was stripped from α-PAI-2 prepared at 3 or 15 μCi/μg, when challenged with a 50-fold molar excess of free diethylenetriaminepentaacetic acid for 45 min in RPMI/5% FCS at 37°C. However, when analyzed by SDS-PAGE, bands representing α-PAI-2 at 15 and 30 μCi/μg were barely visible compared with those representing α-PAI-2 at 0.3 and 3 μCi/μg, although equivalent amounts of protein were loaded in all lanes (Fig. 2A), suggesting protein degradation at these higher specific activities. Autoradiography of the gels showed an increase in the intensity of radioactive degradation products at the bottom of the gel with increasing specific activities of α-PAI-2 (Fig. 2B). All of this corresponded with the observation of maximal uPA/PAI-2 complex formation using α-PAI-2 at 0.3 or 3 μCi/μg (note that bands representing uncomplexed α-PAI-2 were barely evident in the audioradiogram; Fig. 2B). This indicates that specific activities of α-PAI-2 >3 μCi/μg result in inactive and/or partially degraded PAI-2 protein. Indeed, the cytotoxicity of equivalent radioactive doses of α-PAI-2 against MDA-MB-231 cells decreased with increasing specific activity (Fig. 2C). Therefore, α-PAI-2 at a specific activity of 3 μCi/μg was selected for preclinical assessment in mice.

Toxicologic Evaluation of α-PAI-2

Single-Dose Tolerance Evaluation. A single-dose administration of α-PAI-2 at 12.6, 19.5, or 25.8 mCi/kg did not reach toxicity end points (Fig. 3A). A small acute weight loss of 5% to 8% from day 0 was observed in all cohorts; however, this was quickly recovered by day 14 with all mice gaining weight thereafter. Animals in the control and 25.8 mCi/kg cohort were monitored for 84 days posttreatment (data not shown) and no signs of delayed toxicity were observed. There were no macroscopic signs of chronic toxicity to major organs from any of these animals. There was also no macroscopic signs of acute organ toxicity from mice sacrificed 3 and 7 days after administration of ~24 mCi/kg α-PAI-2. We also assessed the toxicity of higher single doses of α-PAI-2 compared with free ^{213}Bi by analyzing the weight changes from a cohort of mice prepared for efficacy studies during the period in which their tumors were not yet established (Fig. 3B). For direct comparison to the single-dose studies above, a 24 mCi/kg α-PAI-2 dose was included (Fig. 3B). This showed that the presence of an early tumor xenograft did not have a significant effect on the mean weight changes, which was <10% from day 0. Furthermore, as only 10% of mice given 34.8 mCi/kg α-PAI-2 reached toxicity end points of 15% weight loss (Fig. 3B), and none showed other signs of distress, the MTD was not reached. In contrast, 50% of mice given 36 mCi/kg free ^{213}Bi reached toxicity end points of 15% weight loss (Fig. 3B). Moreover, other toxicity end points (hunched posture, lack of activity and grooming, and poor skin coloration) were clearly evident in the free ^{213}Bi cohort, even at day 15 when there was no longer any weight differences between the free ^{213}Bi and highest dose α-PAI-2 cohorts.

Multiple Fractionated [Once Daily for 5 Consecutive Days (Daily × 5)] Dose Tolerance Evaluation. Based on the

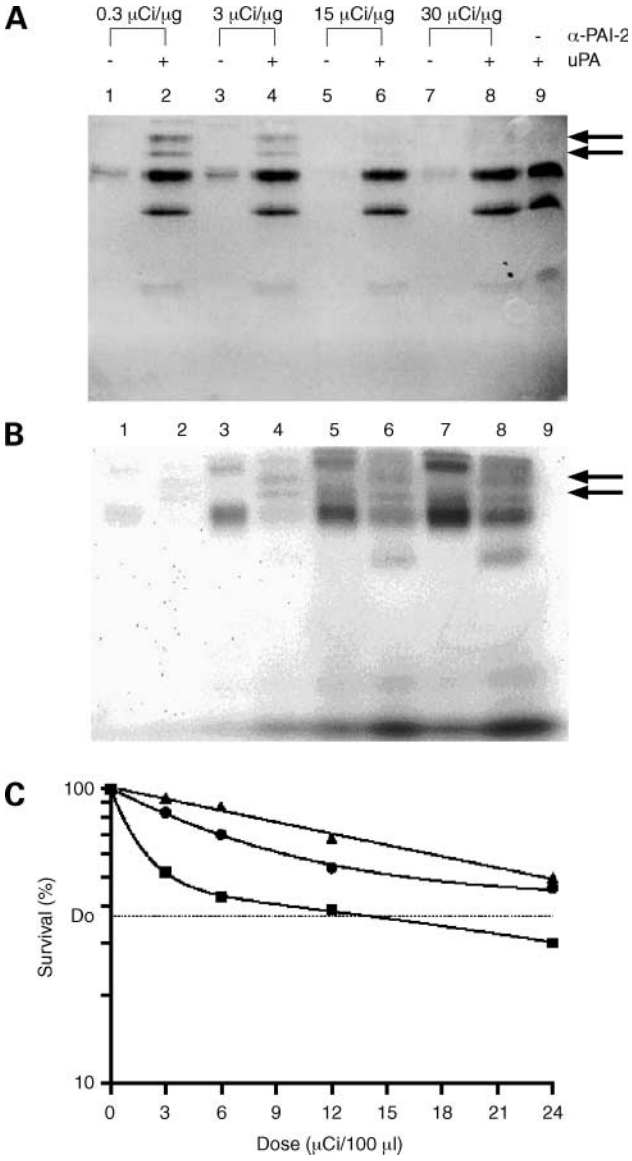

Figure 2. Assessment of α-PAI-2 integrity and uPA-binding ability and *in vitro* cytotoxicity. **A,** equal amounts of PAI-2 protein from α-PAI-2 preparations made at specific activities of 0.3, 3, 15, and 30 μCi/μg were incubated at 37°C for 60 min in the absence or presence of equal amounts of excess uPA; aliquots containing equal protein amounts were fractionated by 12% SDS-PAGE stained using Coomassie blue. **B,** the SDS-PAGE gels were exposed to a phosphor screen for 3 h and scanned using the Storm scanner (GE Healthcare, Fairfield, CT) before Coomassie blue staining. *Odd lanes,* α-PAI-2 alone; *even lanes,* α-PAI-2/uPA complexes; *lane 9,* uPA alone showing the presence of high molecular weight (55 kDa) and low molecular weight (33 kDa) forms of uPA. *Arrows,* complexes between α-PAI-2 and high and low molecular weight uPA. **C,** MDA-MB-231 cells were detached and treated with the specified doses of α-PAI-2 prepared at 3 μCi/μg (■), 15 μCi/μg (●), and 30 μCi/μg (▲). For each dose of the different specific activities, the corresponding control treatment received the same volume of elution buffer and the same amount of unlabeled PAI-2-DTTA. Survival was determined after overnight treatment compared with these controls. *Points,* mean (n = 3); *bars,* SE. Survival plots of MDA-MB-231 cells were fitted to one-phase exponential decay models. Models were selected according to the best fit; none of the data deviated from the fitted model as judged by tests done by GraphPad software. *Dotted line,* Do (37% survival).

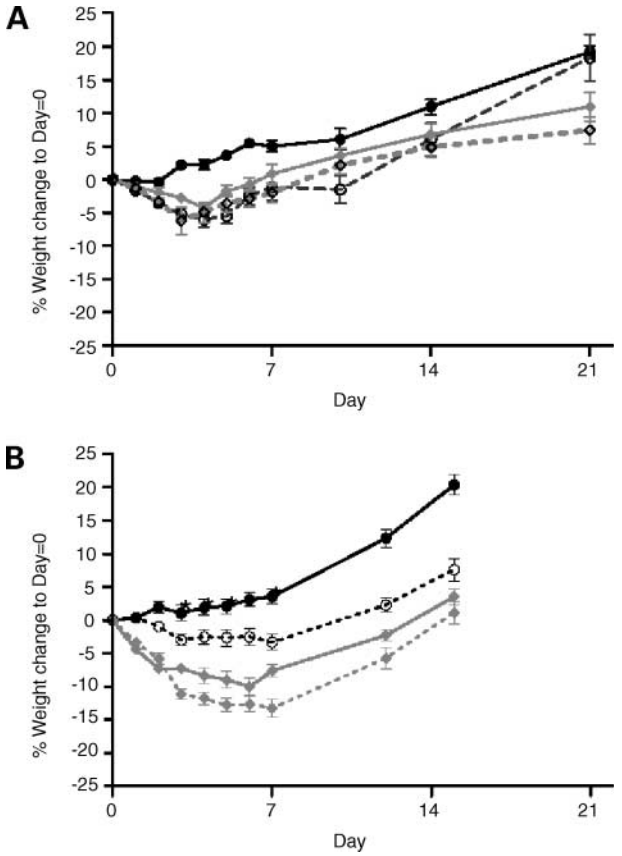

Figure 3. Dose-tolerance relationship for escalating single-dose administration of α-PAI-2 in mice. Average percentage weight changes compared with day 0 (i.e., day of α-PAI-2 administration). **A,** dose-tolerance relationship for mice without tumors. Control (buffer alone; ●, *black line*), 12.6 ± 0.3 mCi/kg α-PAI-2 (○, *black dashed line*), 19.5 ± 0.3 mCi/kg α-PAI-2 (◆, *gray line*), and 25.8 ± 0.6 mCi/kg α-PAI-2 (◇, *gray dashed line*). *Points,* mean (n = 4, 3, 6, and 6, respectively); *bars,* SE. **B,** dose-tolerance relationship for mice with tumor xenografts that were not yet palpable (i.e., treatments were administered 7 d post tumor cell inoculation). Control (buffer alone; ●, *black line*), 24.0 ± 0.6 α-PAI-2 (○, *black dashed line*), 34.8 ± 0.3 α-PAI-2 (◆, *gray line*), and 36.0 ± 0.3 mCi/kg ^{213}Bi (◇, *gray dashed line*). *Points,* mean (n = 10 in each cohort); *bars,* SE. *, $P < 0.05$, values at which all cohorts are significantly different from each other at specific time points.

single-dose toxicologic results, a daily ×5 dose administration schedule of α-PAI-2 at 1.2, 2.43, 3.72, 4.8, or 6.0 mCi/kg/d underwent toxicologic evaluation. Doses of 4.8 mCi/kg/d × 5 or lower did not reach MTD as only average acute minor weight losses of <10%, which were recovered within 7 to 10 day of the last α-PAI-2 administration, were noted (Fig. 4A). This corresponded with the lack of toxicity observed with the single bolus dose of 25.8 mCi/kg α-PAI-2. However, it is likely that the MTD for this multiple-dose schedule lies between 4.8 and 6.0 mCi/kg/d × 5 α-PAI-2 as 9 of 12 mice in the 6.0 mCi/kg/d × 5 cohort reached the end point of 15% weight loss (Fig. 4A).

The multiple-dose administration schedule was assessed against the HI/citrate/PBS buffer, PAI-2-DTTA, ^{213}Bi, and no-injection controls to determine the toxicity of the individual components of α-PAI-2 as well as the treatment schedule. The no-injection cohort was simply handled daily as per the treatment cohorts. There was no significant difference between any of these controls, excluding ^{213}Bi (Fig. 4B). This indicates that PAI-2-DTTA was not toxic and any weight loss may be attributed to injection stress/handling, which was minor and quickly recovered. Comparison of equivalent doses of 6.0 mCi/kg/d × 5 of α-PAI-2 (Fig. 4A) to ^{213}Bi (Fig. 4B) indicated that the latter caused larger acute weight losses (minus 15–20% for all mice), which were not regained by the end of the observation period ($P < 0.05$ at day 25). The ^{213}Bi cohort also showed signs of distress, such as hunched posture and a gray skin coloration throughout.

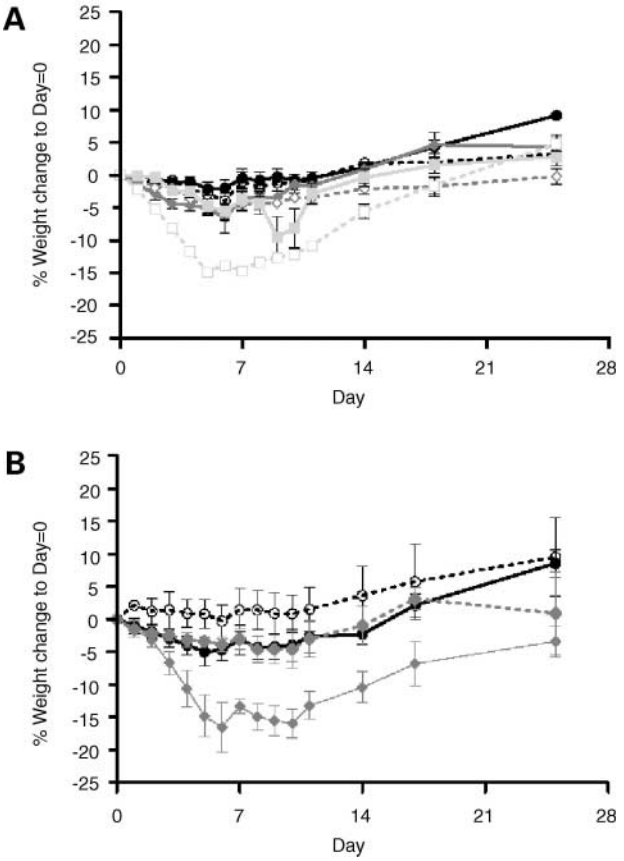

Figure 4. Dose-tolerance relationship for escalating multiple fractionated daily ×5 dose administration schedule of α-PAI-2 (**A**), and comparison of toxicity of individual components within the α-PAI-2 formula (**B**) in mice. Animals received daily treatments on days 0 to 4 and the average percentage weight changes compared with day 0 are shown. **A,** the % weight changes from day 0 for each mouse are shown for the control (buffer alone) cohort (●, *black line*), and the 1.2 ± 0.03 mCi/kg/d (○, *black dashed line*), 2.43 ± 0.03 mCi/kg/d (◆, *gray line*), 3.72 ± 0.09 mCi/kg/d (◇, *gray dashed line*), 4.80 ± 0.12 mCi/kg/d (■, *light gray line*), and 6.0 ± 0.06 mCi/kg/d (□, *light gray dashed line*) ×5 α-PAI-2 cohorts. *Points,* mean (n = 13, 6, 3, 6, 6, and 12, respectively); *bars,* SE. **B,** the % weight change from day 0 for each mouse are shown for the control (buffer alone) cohort (●, *black line*), the no injection control (○, *black dashed line*), the 6.0 ± 0.06 mCi/kg/d ^{213}Bi cohort (◆, *gray line*), and the 2.2 mg/kg/d ×5 PAI-2-DTTA cohort (◇, *gray dashed line*). *Points,* mean (n = 13, 3, 4, and 3, respectively); *bars,* SE.

Histopathologic and Blood Analyses. Histopathologic analysis of major organs (liver, kidney, and spleen) removed from mice in the 6.0 mCi/kg/d × 5 α-PAI-2 cohort at day 30, as well as from mice in the 24 mCi/kg α-PAI-2 cohort at days 3 and 7, confirmed the absence of acute organ toxicity as no abnormalities were evident (data not shown). However, an increase in WBC counts compared with controls was observed at days 3 and 7 after 24 mCi/kg α-PAI-2 administration (3.5- and 1.8-fold, respectively). This suggested either a short-term inflammatory response and/or necrosis due to the treatment, as blood cell counts taken from mice sacrificed 33 to 74 days after 24 or 36 mCi/kg α-PAI-2 administration in either of the treatment cohorts were not significantly different to controls (data not shown). In contrast, mice from the 36 mCi/kg ^{213}Bi cohort showed signs of distress. This included evidence of failing renal function (e.g., urea levels 5-fold higher than controls) and liver dysfunction potentially associated with relatively modest cell death (e.g., liver enzyme alanine aminotransferase levels 3-fold higher than controls). Histopathologic analysis confirmed liver and kidney damage by ^{213}Bi.

Evaluation of Efficacy of α-PAI-2 against Early (7-Day) and Established (21-Day) MDA-MB-231 Tumor Xenografts

Single-Dose Efficacy against Early (7-Day) Tumors. The effect of a single bolus dose of α-PAI-2 at 24.0 and 34.8 mCi/kg on tumor growth rates and host survival was assessed using the early tumor model. As 25.8 mCi/kg α-PAI-2 did not reach MTD, the higher dose was incorporated for the purposes of observing a dose response for efficacy and extending our knowledge of the toxicity of high single doses of α-PAI-2 (discussed above). Although not significant at all time points nor dose dependent, decreased tumor growth rates in treatment cohorts compared with the control cohort were observed (Fig. 5A). However, compared with controls, a significant survival advantage was conferred by administration of 34.8 mCi/kg but not 24.0 mCi/kg α-PAI-2 (Fig. 5B).

Multiple Fractionated (Daily ×5) Dose Efficacy against Early (7-Day) and Established (21-Day) Tumors. The effect of ~4.8 mCi/kg/d × 5 α-PAI-2 administered from 7 days (Fig. 6A and B) and 21 days (Fig. 6C and D) after tumor cell inoculation against tumor growth rates and host survival were examined. There was a significant delay in the tumor growth rate using either tumor model after completion of this α-PAI-2 administration schedule (Fig. 6A and C), suggesting that α-PAI-2 is equally effective against established (palpable) tumors. Furthermore, in either model, multiple-fractionated-dose administration of α-PAI-2 conferred a significant survival advantage compared with controls (Fig. 6B and D). For example, at day 40 after α-PAI-2 treatment, all animals were alive, whereas 66% of control mice were sacrificed due to reaching tumor size end points (Fig. 6D). Given the lack of toxicity at these doses, it is conceivable that a second dose of α-PAI-2 could be administered at day 40 to prolong survival time.

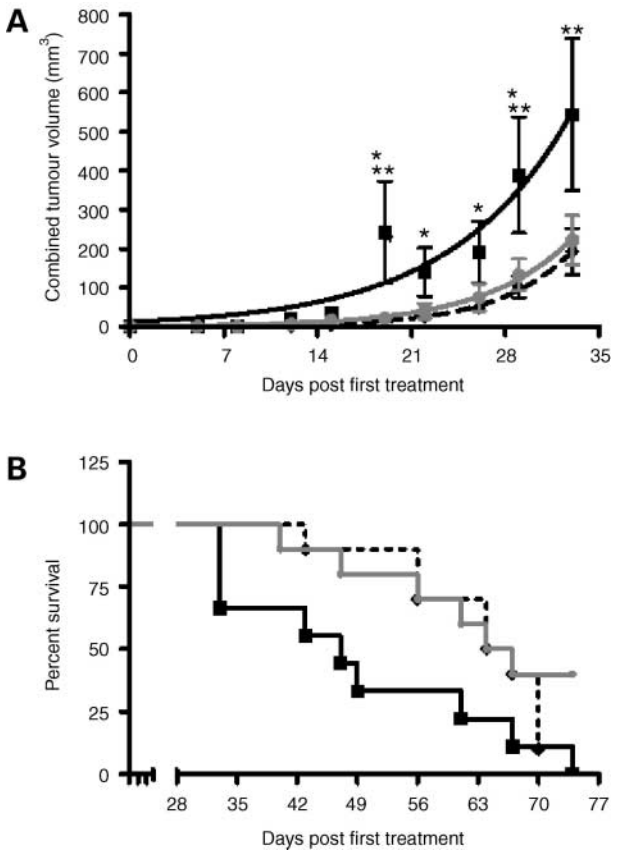

Figure 5. Single-dose dose efficacy against early (7-d) tumors. Mice were inoculated with tumor cells 7 d before administration of α-PAI-2. **A,** the tumor growth rates are shown for the control (buffer alone) cohort (■, *solid black line*, $n = 9$), and the 24.0 ± 0.6 mCi/kg (♦, *black dashed line*, $n = 10$) and 34.8 ± 0.3 mCi/kg (●, *gray line*, $n = 10$) α-PAI-2 cohorts. The graph shows the period until the first animal was sacrificed due to reaching a tumor size end point. *Points,* mean; *bars,* SE. Significance ($P < 0.05$) of control versus 24.0 mCi/kg α-PAI-2 cohort (*) and control versus 34.8 mCi/kg α-PAI-2 cohort (**). **B,** survival plots. Control (buffer alone) cohort (■, *solid black line*), 24.0 mCi/kg (♦, *black dashed line*, log-rank $P = 0.1113$), and 34.8 mCi/kg (●, *gray line*, log-rank $P = 0.0269$) α-PAI-2 cohorts.

Discussion

There is extensive experimental, preclinical, and clinical data that supports the role of the uPA system as a marker of malignancy (2, 3, 13). We have previously shown the potential of α-PAI-2 as an efficacious anti-uPA–targeted therapy against metastatic breast carcinoma models (16–18). Herein, extensive preclinical safety and efficacy evaluation data of α-PAI-2 is described. Variation of the specific activity of 0.3 to 30 μCi/μg had pronounced effects on the α-PAI-2 preparations and their cytotoxicity *in vitro*. At specific activities of ≥15 μCi/μg, α-PAI-2 started to degrade, probably due to radiolysis, and this was likely responsible for the reduced cytotoxicity *in vitro*. The specific activity of 3 μCi/μg was thus selected to conduct the extensive preclinical evaluation of α-PAI-2 as (*a*) this preparation did not affect the structural integrity of PAI-2

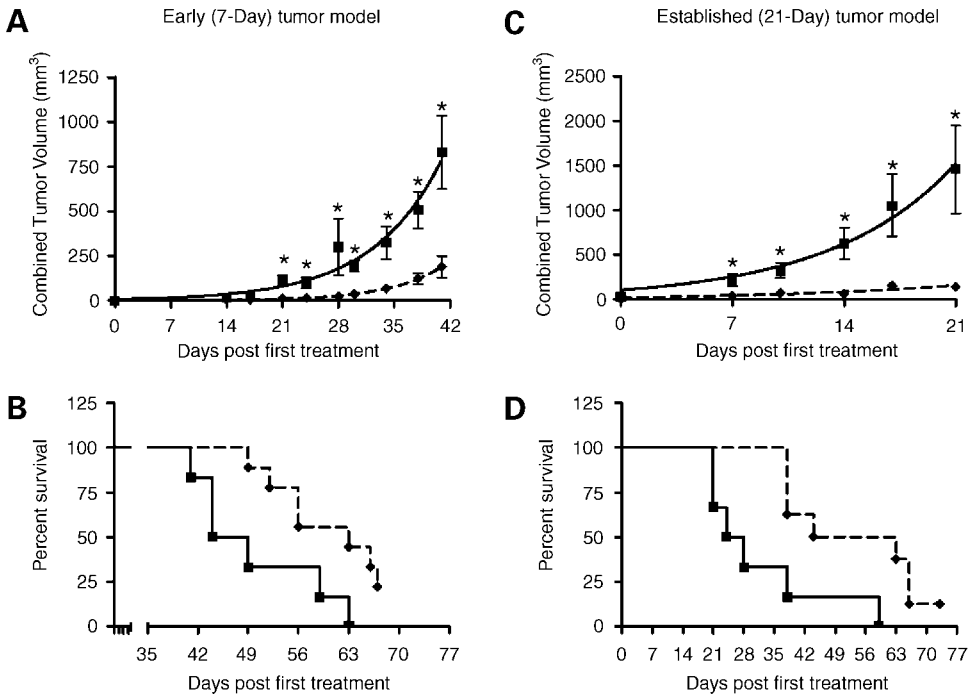

Figure 6. Multiple fractionated (daily ×5) dose efficacy against early (7-d; **A** and **B**) and established (21-d; **C** and **D**) tumors. **A** and **B,** mice were inoculated with tumor cells 7 d before the administration schedule. A dose of 4.86 ± 0.06 mCi/kg was administered daily for 5 d from days 0 to 4. **A,** the tumor growth rates are shown for the control (buffer alone) cohort (■, *black solid line*, $n = 6$) and the 4.86 mCi/kg/d × 5 α-PAI-2 cohort (♦, *black dashed line*, $n = 8$). The graph shows the period until the first animal was sacrificed due to reaching the tumor size end point. *Points,* mean; *bars,* SE. *, $P < 0.05$, significance of control versus 4.86 mCi/kg/d × 5 α-PAI-2 cohorts. **B,** survival plots. Control (■, *black solid line*) and 4.86 mCi/kg/d × 5 α-PAI-2 (♦, *black dashed line*, log-rank $P = 0.0233$) cohorts. **C** and **D,** mice were inoculated with tumor cells 21 d before administration of α-PAI-2. A dose of 4.62 ± 0.06 mCi/kg/d × 5 α-PAI-2 was administered daily for 5 d from days 0 to 4. **C,** the tumor growth rates are shown for the control (buffer alone) cohort (■, *black solid line*, $n = 6$) and the 4.62 ± 0.06 mCi/kg/d × 5 α-PAI-2 cohort (♦, *black dashed line*, $n = 8$). The graph indicates the period until the first animal was sacrificed due to reaching the tumor size end point. *Points,* mean; *bars,* SE. *, $P < 0.05$, significance of control versus 4.62 ± 0.06 mCi/kg/d × 5 α-PAI-2 cohorts. **D,** survival plots. Control (buffer alone) cohort (■, *black solid line*) and 4.62 ± 0.06 mCi/kg/d × 5 α-PAI-2 cohort (♦, *black dashed line*, log-rank $P = 0.0077$).

or its uPA-binding ability and (*b*) ^{213}Bi incorporation was stable, at least over the time frame incorporating ^{213}Bi half-life of 46 min.

We took advantage of the uPA-expressing MDA-MB-231 human tumor cell line to prove the concept of specific receptor-bound uPA targeting by PAI-2 *in vivo*. However, it has been suggested that xenogenic tumor models may not be suitable surrogates for anti–uPA/uPAR targeting strategies in human cancer (4). This is particularly the case for uPAR antagonists as there are significant species specificity differences in the uPA/uPAR interaction (4, 13). However, because human PAI-2 inhibited mouse uPA and was internalized by a murine fibroblastic cell line via receptor-bound uPA in an low-density lipoprotein receptor family–dependent manner, then host tissue and/or host stromal cells expressing active uPA should also internalize α-PAI-2. It is acknowledged that at the probable low concentrations of α-PAI-2 in tissues, the reaction rate may be too slow to allow PAI-2 to act as an efficient inhibitor of murine uPA. For example, from the second-order association rate constants, the calculated time for effective inhibition of mouse uPA by human PAI-2 would be ~70-fold slower than equivalent concentrations of human PAI-2 against human uPA. However, any cytotoxic effect may only require a fraction of the actual enzyme inhibition due to the high cellular toxicity of the α particle emissions. Therefore, the use of a mouse model should provide a reasonable estimation of nonspecific toxicity due to human α-PAI-2.

Thus, the dose-tolerance relationship for both single and multiple fractionated dose administration schedules of α-PAI-2 were examined. Single-dose administration up to 34.8 mCi/kg α-PAI-2 did not reach toxicity end points, indicating that the MTD for a single-dose regimen is >34.8 mCi/kg. Higher single doses of α-PAI-2 were not examined because, based on a body surface area calculation, this dose is higher than that which was possible to administer to humans using [^{213}Bi]CD33 against myeloid leukemia in a phase 1 clinical trial (30). No mice reached toxicity end points when given 4.8 mCi/kg/d × 5 (an accumulated dose of 24 mCi/kg) compared with 75% of mice given 6.0 mCi/kg/d × 5 α-PAI-2 (an accumulated dose of 30 mCi/kg), indicating that the MTD lies between 4.8 and 6.0 mCi/kg/d × 5. However, all animals recovered their pretreatment weights well within the observation period, and abnormal blood and histopathologic variables

of both acute and chronic toxicity to major organs were not evident. Our estimation of the MTD for α-PAI-2 is thus probably conservative, and higher doses per kilogram for the human equivalent MTD should not be ruled out in a clinical trial setting, especially if tumor control cannot be established without 15% weight loss.

The administration of ^{213}Bi alone, using either administration schedule, resulted in greater weight losses that took longer to recover than with the equivalent dose of α-PAI-2. In addition, mice showed other signs of toxicity (chronic kidney and liver dysfunction) not apparent in the α-PAI-2 treatment cohorts. This suggests that PAI-2 targets the radiotoxin to uPA-expressing cells only, thus providing a significant therapeutic advantage. Indeed, the presence of a tumor significantly increases [^{125}I]PAI-2 blood clearance rates compared with tumor-free mice and causes less [^{125}I]PAI-2 to accumulate in the major organs (19), possibly via enhanced binding and degradation of PAI-2 through tumor/stromal cell uPA. Given the potential targeting ability of host (murine) uPA-expressing cells by α-PAI-2, and the lack of significant toxicity in mice, these differences in toxicity further confirm uPA-targeting selectivity and lack of nonspecific toxicity of PAI-2. This also suggests that, as was shown *in vitro*, the majority of ^{213}Bi remains incorporated with PAI-2-DTTA *in vivo*.

A second, nonrodent species is usually chosen for full toxicologic assessment of a new therapeutic before proceeding to human trials. However, as the second-order association rate constants between human PAI-2 and rabbit uPA are of the same magnitude as human PAI-2 and human uPA, rabbits would be an appropriate second species for such studies. Confirmation of the MTD and detailed toxicology should be done in rabbits using the multiple-dose schedule of α-PAI-2 before proceeding to human trials. In addition, whole-body imaging of rabbits treated at the MTD could also be done with α-PAI-2 to provide data for dosimetry calculations as described by McDevitt et al. (31).

Although both single- and multiple-fractionated-dose administration schedules resulted in early tumor growth delay, a survival advantage was not significant for the 25.8 mCi/kg dose compared with the 4.8 mCi/kg/d × 5 dose. Furthermore, the sub-MTD dose of 4.8 mCi/kg/d × 5 α-PAI-2 also conferred a significant survival advantage against established tumors. Using the single-dose schedule, the effect on tumor growth rate was not dose dependent nor was it significantly different from controls at all time points, even at 36 mCi/kg. Thus, the 4.8 mCi/kg/d × 5 dose of α-PAI-2 was the safest and most efficacious schedule against breast carcinoma growth in mice. Because this dose of α-PAI-2 caused little toxicity and did not result in radiation damage to kidneys and livers in mice, a second cycle of treatment could possibly be administered to prolong the survival conferred by α-PAI-2 in tumor-bearing mice.

The fact that the multiple-dose administration schedule tested here did not eradicate tumors may be attributed to the conservative dose used, as well as to an uneven distribution of cell surface uPA expression in this tumor model (as would be expected in human carcinoma) and the short path-length and half-life of ^{213}Bi. Nevertheless, the significant reduction in primary tumor growth is noteworthy because targeted α radionuclides are usually most effective for treating small-volume diseases, such as leukemias and micrometastases, or residual disease post surgical removal of the tumor burden (15, 31, 32). The relatively small size of PAI-2 (47 kDa) may assist tumor penetration (15). It is possible that α-PAI-2 also targeted cell surface uPA–expressing stromal cells in the tumor tissue and that this may have assisted in tumor growth retardation as the stroma is thought to support tumor growth (4, 13, 19). Moreover, there has been growing appreciation for the nontargeted effect of radiation in general (33) and α particles specifically (33–35), referred to as the ''bystander effect.'' This effect is related to the release of enzymes and factors (e.g., cytokines) from directly hit cells that may have a significant biological effect on the surrounding cells (33). Whether α-PAI-2 also initiates this bystander effect in tumors remains to be determined.

Clinical trials using targeted monoclonal antibody approaches and traditional chemotherapy have shown significant synergistic effects leading to much improved outcomes (36). Although efficacious against a primary tumor model as a single agent, we envisage that α-PAI-2 would be most useful as an adjuvant therapy following conventional therapy to prevent invasion and metastasis and control micrometastases without the serious side effects associated with current therapies.

Acknowledgments

We thank Dr. T. Maddocks (University of Wollongong) for assistance with animal experiments and postmortem analyses; Dr. M. Carolan (South Eastern Sydney and Illawarra Area Health Service) for helpful discussions and critical reading of the manuscript; Dr. Martin Copland (IDEXX Laboratories) for assistance with histopathology and blood analyses; Dr. S. Rizvi and Prof. B. Allen for helpful discussions; Dr. N. Behrendt (Finsen Laboratory, Copenhagen, Denmark) for provision of murine uPA and human PAI-1; and PAI-2 Pty Limited (Australia) for providing human recombinant PAI-2.

References

1. Schmitt M, Wilhelm O, Reuning U, et al. The urokinase plasminogen activator system as a novel target for tumour therapy. Fibrinol Proteol 2000;14:114 – 32.

2. Ranson M, Andronicos NM. Plasminogen binding and cancer: promises and pitfalls. Front Biosci 2003;8:s294 – 304.

3. Duffy MJ. The urokinase plasminogen activator system: role in malignancy. Curr Pharm Des 2004;10:39 – 49.

4. Romer J, Nielsen BS, Ploug M. The urokinase receptor as a potential target in cancer therapy. Curr Pharm Des 2004;10:2359 – 76.

5. Ertongur S, Lang S, Mack B, et al. Inhibition of the invasion capacity of carcinoma cells by WX-UK1, a novel synthetic inhibitor of the urokinase-type plasminogen activator system. Int J Cancer 2004;110:815 – 24.

6. Almholt K, Lund LR, Rygaard J, et al. Reduced metastasis of transgenic mammary cancer in urokinase-deficient mice. Int J Cancer 2005;113: 525 – 32.

7. Kruithof EKO, Baker MS, Bunn CL. Biological and clinical aspects of plasminogen activator inhibitor type-2. Blood 1995;86:4007 – 24.

8. Al-Ejeh F, Croucher D, Ranson M. Kinetic analysis of plasminogen activator inhibitor type-2: urokinase complex formation and subsequent internalisation by carcinoma cell lines. Exp Cell Res 2004;297:259 – 71.

9. Silverman GA, Bird PI, Carrell RW, et al. The serpins are an expanding superfamily of structurally similar but functionally diverse proteins. Evolution, mechanism of inhibition, novel functions, and a revised nomenclature. J Biol Chem 2001;276:33293 – 6.

10. Kjoller L. The urokinase plasminogen activator receptor in the regulation of the actin cytoskeleton and cell motility. Biol Chem 2002; 383:5 – 19.

11. Weigelt B, Peterse JL, van 't Veer LJ. Breast cancer metastasis: markers and models. Nat Rev Cancer 2005;5:591 – 602.

12. Bhowmick NA, Neilson EG, Moses HL. Stromal fibroblasts in cancer initiation and progression. Nature 2004;432:332 – 7.

13. Dano K, Behrendt N, Hoyer-Hansen G, et al. Plasminogen activation and cancer. Thromb Haemost 2005;93:676 – 81.

14. Liu S, Aaronson H, Mitola DJ, Leppla SH, Bugge TH. Potent antitumor activity of a urokinase-activated engineered anthrax toxin. Proc Natl Acad Sci U S A 2003;100:657 – 62.

15. Robinson MK, Weiner LM, Adams GP. Improving monoclonal antibodies for cancer therapy. Drug Dev Res 2004;61:172 – 87.

16. Ranson M, Tian Z, Andronicos NM, Rizvi S, Allen BJ. *In vitro* cytotoxicity of bismuth-213 (213Bi)-labeled-plasminogen activator inhibitor type 2 (α-PAI-2) on human breast cancer cells. Breast Cancer Res Treat 2002;71:149 – 59.

17. Li Y, Rizvi SM, Ranson M, Allen BJ. ^{213}Bi-PAI2 conjugate selectively induces apoptosis in PC3 metastatic prostate cancer cell line and shows anti-cancer activity in a xenograft animal model. Br J Cancer 2002;86: 1197 – 203.

18. Allen BJ, Tian Z, Rizvi SM, Li Y, Ranson M. Preclinical studies of targeted α therapy for breast cancer using ^{213}Bi-labelled-plasminogen activator inhibitor type 2. Br J Cancer 2003;88:944 – 50.

19. Hang MTN, Ranson M, Saunders DN, et al. Pharmacokinetics and biodistribution of recombinant human plasminogen activator inhibitor type 2 (PAI-2) in control and tumour xenograft-bearing mice. Fibrinol Proteol 1998;12:145 – 54.

20. Croucher D, Saunders DN, Ranson M. The urokinase/PAI-2 complex: A new high affinity ligand for the endocytosis receptor LRP. J Biol Chem 2006;281:10206 – 13.

21. McDevitt MR, Sgouros G, Finn RD, et al. Radioimmunotherapy with α-emitting nuclides. Eur J Nucl Med 1998;25:1341 – 51.

22. Ranson M, Andronicos NM, O'Mullane MJ, Baker MS. Increased plasminogen binding is associated with metastatic breast cancer cells: differential expression of plasminogen binding proteins. Br J Cancer 1998; 77:1586 – 97.

23. Andronicos NM, Ranson M. The topology of plasminogen binding and activation on the surface of human breast cancer cells. Br J Cancer 2001; 85:909 – 16.

24. Williams JW, Morrison JF. The kinetics of reversible tight-binding inhibition. Methods Enzymol 1979;63:437 – 67.

25. Allen BJ, Raja C, Rizvi S, et al. Intralesional targeted α therapy for metastatic melanoma. Cancer Biol Ther 2005;4:1318 – 24.

26. Perry MC. Chemotherapy source book. Philadelphia: Lippincott, Williams and Wilkins; 2001.

27. Jessani N, Humphrey M, McDonald WH, et al. Carcinoma and stromal enzyme activity profiles associated with breast tumor growth *in vivo*. Proc Natl Acad Sci U S A 2004;101:13756 – 61.

28. Allen BJ, Rizvi S, Li Y, Tian Z, Ranson M. *In vitro* and preclinical targeted α therapy for melanoma, breast, prostate and colorectal cancers. Crit Rev Oncol Hematol 2001;39:139 – 46.

29. Solberg H, Ploug M, Hoyer-Hansen G, Nielsen BS, Lund LR. The murine receptor for urokinase-type plasminogen activator is primarily expressed in tissues actively undergoing remodeling. J Histochem Cytochem 2001;49:237 – 46.

30. Jurcic JG, Larson SM, Sgouros G, et al. Targeted α particle immunotherapy for myeloid leukemia. Blood 2002;100:1233 – 9.

31. McDevitt MR, Barendswaard E, Ma D, et al. An α-particle emitting antibody ([213Bi]J591) for radioimmunotherapy of prostate cancer. Cancer Res 2000;60:6095 – 100.

32. Mulford DA, Scheinberg DA, Jurcic JG. The promise of targeted {α}-particle therapy. J Nucl Med 2005;46 Suppl 1:199 – 204S.

33. Hall EJ. The bystander effect. Health Phys 2003;85:31 – 5.

34. Belyakov OV, Malcolmson AM, Folkard M, Prise KM, Michael BD. Direct evidence for a bystander effect of ionizing radiation in primary human fibroblasts. Br J Cancer 2001;84:674 – 9.

35. Shao C, Furusawa Y, Kobayashi Y, Funayama T, Wada S. Bystander effect induced by counted high-LET particles in confluent human fibroblasts: a mechanistic study. FASEB J 2003;17:1422 – 7.

36. Chabner BA, Roberts TG, Jr. Timeline: Chemotherapy and the war on cancer. Nat Rev Cancer 2005;5:65 – 72.

Molecular Cancer Therapeutics

Preclinical evaluation of ^{213}Bi-labeled plasminogen activator inhibitor type 2 in an orthotopic murine xenogenic model of human breast carcinoma

Tamantha K. Stutchbury, Fares Al-ejeh, Gillian E. Stillfried, et al.

Mol Cancer Ther 2007;6:203-212.